Creep Relaxation of Nonaxisymmetric Thermal Stresses in Thick Walled Cylinders

M. SABBAGHIAN*
Louisiana State University, Baton Rouge, La.
AND
M. R. ESLAMI†
Tehran Polytechnic, Tehran, Iran

Thermal stresses in thick walled cylinders subjected to nonaxisymmetric thermal boundary conditions are ascertained. Based on these initial stresses and the material's creep property, time-dependent thermal stress equations are derived. For the analysis, effective stress and strain rate and the power function creep law are used in conjunction with the relaxation and equilibrium equations. Dimensionless stresses are plotted for one thermal boundary condition. Parameters for several other thermal boundary conditions are provided so that they can be extrapolated for other cases. A practical numerical procedure is presented that is applicable in most cases. In this investigation, the material's creep property is assumed to be 1) constant, and 2) temperature dependent. It has been shown that the relaxation rate differs in the case of a vessel with temperature-dependent creep properties from that with constant creep properties.

Nomenclature

a	= inside radius of cylinder
A_1	= constant depending on thermal boundary condition
b	= outside radius of cylinder
B	= material's creep property
B_o	= constant depending on thermal boundary condition
E	= elastic modus
k	= thermal conductivity
n	= material's creep property
n_1, n_2	= material's creep constants for temperature dependent creep property
q	= heat flow rate per unit surface area
r	= radius
t	= time
t_p	= time parameter
T	= temperature
T_1	= temperature at $r = b$ and $-\beta < \phi < +\beta$
T_2	= temperature at $r = b$ and $\beta < \phi < \pi, -\pi < \phi < -\beta$
T_i	= inside temperature
α	= thermal expansion coefficient
ν	= Poisson's ratio
$\varepsilon_r, \varepsilon_\phi, \varepsilon_z$	= radial, tangential, and axial strains
$\dot{\varepsilon}$	= strain rate
$\varepsilon_e{}^*$	= effective elastic strain
$\varepsilon_c{}^*$	= effective creep strain
$\sigma_r, \sigma_\phi, \sigma_z$	= radial, tangential, and axial stresses
$\sigma_{r_o}, \sigma_{\phi_o}, \sigma_{z_o}$	= original radial, tangential, and axial stresses
σ^*	= effective stress

Introduction

CREEP and relaxation at elevated temperature is a common design problem in many areas of engineering. The increasing interest in high pressure and temperature in many applications has called attention to creep properties of metals. High operating temperature level is generally associated with high temperature gradients and thermal stresses, while at the same time reducing the strength of material. Mechanical and thermal stresses considered in the design of structural components can become a misleading factor when predicting the behavior and service life of the component if one does not take into account the change in stresses due to creep relaxation. Therefore, it becomes necessary to analyze the mechanism of changes that take place, with time, as the result of these stresses.

Cylindrical vessels are one of the common structural components in many industrial applications. In most cases—whether the cylinder is used as a container or heating or cooling reactor—the thermal boundary conditions are not axisymmetric, therefore causing nonaxisymmetric thermal stresses in the vessel. In this paper, the creep relaxation of nonaxisymmetric thermal stresses in cylindrical vessels is analyzed and a numerical method is presented that can be employed to predict the thermal stresses in terms of time.

Nonaxisymmetric thermal stresses in cylinders have been discussed by many investigators including Morozov and Fridman,[1] Zudans, Yen, and Steigelmann[2] and Boley and Weiner.[3] These stresses, particularly at high temperatures, result in the creep process. The subject of creep at elevated temperatures has been treated by Wahl,[4] Baily,[5] Rabatnov,[6] and McVetty,[7] just to name a few. The effect of creep when the total strain (the sum of elastic and creep strain) remains constant is to relax and moderate the elastic strains and stresses. It would be more realistic, and in critical cases necessary, to include the effect of creep relaxation in the analysis of stresses.

Uniaxial stress relaxation is discussed by Nadai and Davis.[8] Griffith and Marin[9] considered the stress relaxation under combined state of stress and Sabbaghian[10] applied the stress relaxation principle to the case of multilayered cylinders.

Analysis of creep and stress relaxation under the combined state of stress is usually of such a nature that a numerical technique becomes useful. Mendelson[11] has formulated a general approach for the numerical solution of creep problems. Recently, Sabbaghian and Eslami[12] proposed a general numerical procedure for the solution of stress relaxation problems and applied the method to the case of cylinders subjected to axisymmetric thermal stresses. The research reported in this paper is an extension of work done in Ref. 12. Here the method is applied to nonaxisymmetric thermal stresses.

Received February 7, 1974; revision received June 14, 1974.
Index category: Thermal Stresses.

* Professor, Mechanical, Aerospace and Industrial Engineering Department.
† Assistant Professor, Mechanical Engineering Department.

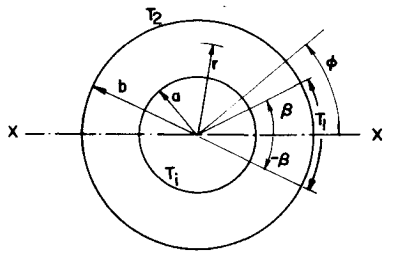

Fig. 1 The thick walled cylinder.

Nonaxisymmetric Temperature Distribution in Cylinders

Consider a cylinder with inside and outside radii a and b, respectively, as shown in Fig. 1. Temperature is assumed to be constant along the axis of cylinder and in a steady-state condition. Furthermore, temperature at the inside surface of cylinder T_i is circumferentially uniform while part of the outside surface of cylinder ($-\beta < \phi < \beta$) is subjected to temperature T_1 and the rest is subjected to T_2. The coordinate axes can always be chosen in such a manner that the plane containing the line X-X and the cylinder axis be a plane of symmetry for temperature field. In such a case only half of the cylinder needs to be considered. Thus the Laplace equation

$$\frac{\partial^2\theta}{\partial r^2}+\frac{1}{r}\frac{\partial\theta}{\partial r}+\frac{1}{r^2}\frac{\partial^2\theta}{\partial\phi^2}=0 \tag{1}$$

in which $\theta = T - T_i$ is to be solved subjected to the boundary conditions

$$\begin{aligned}&\theta(a,\phi)=0 \qquad 0<\phi<\pi\\ &\partial\theta/\partial\phi=0 \quad \text{at} \quad \phi=0,\ a\leqq r\leqq b\\ &\partial\theta/\partial\phi=0 \quad \text{at} \quad \phi=\pi,\ a\leqq r\leqq b\\ &\theta(b,\phi)=\begin{cases}T_1-T_i=T_1' & 0<\phi<\beta\\ T_2-T_i=T_2' & \beta<\phi<\pi\end{cases}\end{aligned} \tag{2}$$

The general solution of Eq. (1)

$$\theta(r,\phi)=A_o+B_o\ln r+\sum_\lambda\left[A_\lambda(r/a)^\lambda+B_\lambda(r/a)^{-\lambda}\right]\cos\lambda\phi+\sum_\lambda\left[C_\lambda(r/a)^\lambda+D_\lambda(r/a)^{-\lambda}\right]\sin\lambda\phi \tag{3}$$

can be reduced, using the first three boundary conditions, to

$$\theta(r,\phi)=B_o\ln\frac{r}{a}+\sum_{m=1}^{\infty}A_m\left[\left(\frac{r}{a}\right)^m-\left(\frac{r}{a}\right)^{-m}\right]\cos m\phi \tag{4}$$

Substituting the fourth boundary condition into Eq. (4) gives

$$\theta(b,\phi)=B_o\ln\frac{b}{a}+\sum_{m=1}^{\infty}A_m\left[\left(\frac{b}{a}\right)^m-\left(\frac{b}{a}\right)^{-m}\right]\cos m\phi \tag{5}$$

Using T_1', defined in Eq. (2), as the reference for $\theta(b,\phi)$ and then normalizing θ through division by $(T_2'-T_1')$, Eq. (5) results in

$$\bar\theta'(b,\phi)=\frac{\theta(b,\phi)-T_1'}{T_2'-T_1'}=\frac{B_o\ln(b/a)-T_1'}{T_2'-T_1'}+\sum_{m=1}^{\infty}\frac{A_m}{T_2'-T_1'}\left[\left(\frac{b}{a}\right)^m-\left(\frac{b}{a}\right)^{-m}\right]\cos m\phi \tag{6}$$

where

$$\theta'(b,\phi)=\begin{cases}0 & 0<\phi<\beta\\ 1 & \beta<\phi<\pi\end{cases} \tag{7}$$

To calculate the constants B_o and A_m, one can take advantage of the Fourier series. The Fourier expansion of a step function defined by Eq. (7) is

$$\theta'(b,\phi)=\frac{\pi-\beta}{\pi}+\frac{2}{\pi}\sum_{m=1}^{\infty}\frac{(-1)^m}{m}\sin m(\pi-\beta)\cos m\phi \tag{8}$$

Comparing Eqs. (6) and (8) in conjunction with the last condition given in Eq. (2) yields

$$B_o=\{(T_2-T_i)-(T_2-T_1)(\beta/\pi)\}/\ln(b/a) \tag{9}$$

$$A_m=\frac{2(-1)^m\sin m(\pi-\beta)}{m\pi}\frac{T_2-T_1}{(b/a)^m-(b/a)^{-m}} \tag{10}$$

Substituting B_o and A_m into Eq. (4) and considering the definition of θ, the equation of temperature distribution in cylinder becomes

$$T(r,\phi)=T_i+\frac{(T_2-T_i)-(T_2-T_1)(\beta/\pi)}{\ln\frac{b}{a}}\ln\frac{r}{a}+\frac{2(T_2-T_1)}{\pi}\sum_{m=1}^{\infty}\frac{(-1)^m\sin n(\pi-\beta)}{m}\frac{(r/a)^m-(r/a)^{-m}}{(b/a)^m-(b/a)^{-m}}\cos m\phi \tag{11}$$

Coefficients B_o and A_m for several other thermal boundary conditions are given in Table 1.

Initial Thermal Stresses in Cylinder

Thermal stresses due to axisymmetric part of the temperature are

$$\begin{aligned}\sigma'_{r_0}&=\frac{E\alpha}{1-\nu}\left[\frac{1-a^2/r^2}{b^2-a^2}\int_a^b Tr\,dr-\frac{1}{r^2}\int_a^r Tr\,dr\right]\\ \sigma'_{\phi_0}&=\frac{E\alpha}{1-\nu}\left[\frac{1+a^2/r^2}{b^2-a^2}\int_a^b Tr\,dr+\frac{1}{r^2}\int_a^b Tr\,dr-T\right]\end{aligned} \tag{12}$$

Where upon substitution of axisymmetric part of temperature, the first two terms in Eq. (11), and integration, considering the stresses at the boundaries, $\sigma_r = 0$ at $r = a$ and b, one obtains

$$\begin{aligned}\sigma'_{r_0}&=\frac{E\alpha B_o}{2(1-\nu)}\left[\frac{b^2}{b^2-a^2}\left(1-\frac{a^2}{r^2}\right)\ln\frac{b}{a}-\ln\frac{r}{a}\right]\\ \sigma'_{\phi_0}&=\frac{E\alpha B_o}{2(1-\nu)}\left[\frac{b^2}{b^2-a^2}\left(1+\frac{a^2}{r^2}\right)\ln\frac{b}{a}-\ln\frac{r}{a}-1\right]\\ \tau'_{r\phi_0}&=0\end{aligned} \tag{13}$$

The only term in nonaxisymmetric part of temperature distribution that contribute to thermal stresses is $(-1)^m A_m(r/a)^{-m}\cos m\phi$ with $m = 1$. Thermal stresses due to this term are given in Ref. 1 as follows:

$$\begin{aligned}\sigma''_{r_0}&=\frac{E\alpha}{2(1-\nu)}\frac{r}{b^2+a^2}\left(1-\frac{a^2}{r^2}\right)\left(1-\frac{b^2}{r2}\right)A_1\cos\phi\\ \sigma''_{\phi_0}&=\frac{E\alpha}{2(1-\nu)}\frac{r}{b^2+a^2}\left(3-\frac{b^2+a^2}{r^2}-\frac{a^2b^2}{r^4}\right)A_1\cos\phi\\ \tau''_{r\phi_0}&=\frac{E\alpha}{2(1-\nu)}\frac{r}{b^2+a^2}\left(1-\frac{a^2}{r^2}\right)\left(1-\frac{b^2}{r^2}\right)A_1\sin\phi\end{aligned} \tag{14}$$

The total initial stresses in cylinder are, therefore, sum of the corresponding equations in Eqs. (13) and (14). That is

$$\begin{aligned}\sigma_{r_0}&=\sigma'_{r_0}+\sigma''_{r_0}\\ \sigma_{\phi_0}&=\sigma'_{\phi_0}+\sigma''_{\phi_0}\\ \tau_{r\phi_0}&=\tau'_0+\tau''_0\end{aligned} \tag{15}$$

The initial axial stress σ_{z_0} for an axially unrestricted cylinder can be obtained from

$$\sigma_{z_0}=\sigma_{r_0}+\sigma_{\phi_0} \tag{16}$$

In Eqs. (12–16) subscript "0" is used to indicate that these stresses are at time equal zero. As time changes the stresses will change due to material's relaxation. Thus, the initial stresses are completely defined in terms of coefficients B_o and A_1 that depend on thermal boundary conditions. Using the coefficient given in Table 1 in conjunction with Eq. (4) and (13–16), one can readily obtain the nonaxisymmetric temperature as well as thermal stresses in a cylinder for the corresponding boundary condition.

Table 1 Coefficients for different thermal boundary conditions

Thermal boundary condition at $r = b$[a]		Coefficients B_o and A_m to be used in Eqs. (4, 13, and 14)	
		B_o	A_m
1) Heat flow rate $q = \begin{cases} q_1 \\ q_2 \end{cases}$	$0 < \phi < \beta$ $\beta < \phi < \pi$	$\left[(q_2 - q_1)\frac{\beta}{\pi} - q_2\right]\frac{b}{k}$	$\frac{2b(q_1 - q_2)(-1)^m \sin m(\pi - \beta)}{m^3 \pi k \left[\left(\frac{b}{a}\right)^m + \left(\frac{b}{a}\right)^{-m}\right]}$
2) $T(b, \phi) = T_1 + \frac{T_2 - T_1}{\pi}\phi$	$0 < \phi < \pi$	$\frac{T_2 + T_1 - 2T_i}{2 \ln \frac{b}{a}}$	$\frac{-4(T_2 - T_1)}{m^2\pi^2\left[\left(\frac{b}{a}\right)^m - \left(\frac{b}{a}\right)^{-m}\right]}$ $m = 1, 3, 5, 7 \ldots$
3) $q = q_1 + \frac{q_2 - q_1}{\pi}\phi$	$0 < \phi < \pi$	$\frac{-b}{2k}(q_2 + q_1)$	$\frac{4(q_2 - q_1)b}{\pi^2 k m^3\left[\left(\frac{b}{a}\right)^m + \left(\frac{b}{a}\right)^{-m}\right]}$ $m = 1, 3, 5, 7 \ldots$
4) $T(b, \phi) = \begin{cases} T_1 + \frac{T_2 - T_1}{\beta}\phi \\ T_2 \end{cases}$	$0 < \phi < \beta$ $\beta < \phi < \pi$	$\left[T_2 - T_i - \frac{\beta}{2\pi}(T_2 - T_1)\right] \Big/ \ln \frac{b}{a}$	$\frac{2(T_2 - T_1)[(-1)^m \cos m(\pi - \beta) - 1]}{\pi\beta m^2\left[\left(\frac{b}{a}\right)^m - \left(\frac{b}{a}\right)^{-m}\right]}$
5) $q = \begin{cases} q_1 + \frac{q_2 - q_1}{\beta}\phi \\ q_2 \end{cases}$	$0 < \phi < \beta$ $\beta < \phi < \pi$	$\left[(q_2 - q_1)\frac{\beta}{2\pi} - q_2\right]\frac{b}{k}$	$\frac{2(q_1 - q_2)b\,(-1)^m \cos m(\pi - \beta) - 1}{\beta k \pi m^3\left[\left(\frac{b}{a}\right)^m + \left(\frac{b}{a}\right)^{-m}\right]}$
6) $T(b, \phi) = \begin{cases} T_1 \\ T_1 + \frac{T_2 - T_1}{\pi - 2\beta}(\phi - \beta) \\ T_2 \end{cases}$	$0 < \phi < \beta$ $\beta < \phi < \pi - \beta$ $\pi - \beta < \phi < \pi$	$\frac{T_2 + T_1 - 2T_i}{2 \ln \frac{b}{a}}$	$\frac{-4(T_2 - T_1)}{m^2\pi(\pi - 2\beta)}\frac{\cos m\beta}{\left(\frac{b}{a}\right)^m - \left(\frac{b}{a}\right)^{-m}}$
7) $q = \begin{cases} q_1 \\ q_1 + \frac{q_2 - q_1}{\pi - 2\beta}(\phi - \beta) \\ q_2 \end{cases}$	$0 < \phi < \beta$ $\beta < \phi < \pi - \beta$ $\pi - \beta < \phi < \pi$	$\frac{q_2 + q_1}{2}\frac{b}{k}$	$\frac{4(q_2 - q_1)b}{\pi(\pi - 2\beta)km^3}\frac{\cos m\beta}{\left(\frac{b}{a}\right)^m + \left(\frac{b}{a}\right)^{-m}}$

[a] Other boundary conditions are same as those given by the first three conditions in Eq. (2).

Stress Relaxation

Whenever combined state of stress exist, the effective stress and strain rate govern the creep process. They are defined, for plane strain condition, as

$$\sigma_c^* = \frac{1}{(2)^{1/2}}[(\sigma_\phi - \sigma_r)^2 + (\sigma_r - \sigma_z)^2 + (\sigma_z - \sigma_\phi)^2 + 6\tau_{r\phi}^2]^{1/2}$$
$$\dot{\varepsilon}_c^* = \frac{(2)^{1/2}}{3}[(\dot{\varepsilon}_\phi - \dot{\varepsilon}_r)^2 + (\dot{\varepsilon}_r - \dot{\varepsilon}_z)^2 + (\dot{\varepsilon}_z - \dot{\varepsilon}_\phi)^2 + 6\dot{\gamma}_{r\phi}^2]^{1/2} \quad (17)$$

For most applications, the steady-state creep strain is large compared to the primary creep strain. Thus, neglecting the transient creep, the steady-state creep relationship between effective stress and strain rate becomes

$$\dot{\varepsilon}_c^* = B\sigma^{*n} \quad (18)$$

where B and n are material's creep constants. For most materials, B remains almost constant with change in temperature while n is a temperature dependent parameter.

The effective elastic stress and strain, corresponding to those in Eq. (17) for creep, are

$$\sigma_e^* = \frac{1}{(2)^{1/2}}[(\sigma_\phi - \sigma_r)^2 + (\sigma_r - \sigma_z)^2 + (\sigma_z - \sigma_\phi) + 6\tau_{r\phi}^2]^{1/2}$$
$$\varepsilon_e^* = \frac{(2)^{1/2}}{3}[(\varepsilon_\phi - \varepsilon_r)^2 + (\varepsilon_r - \varepsilon_z)^2 + (\varepsilon_z - \varepsilon_\phi)^2 + 6\gamma_{r\phi}^2]^{1/2} \quad (19)$$

Employing the elastic stress-strain equations and considering that

$$\sigma_z = \sigma_r + \sigma_\phi \quad (20)$$

the relationship between the effective elastic stress and strain becomes

$$\varepsilon_e^* = \frac{2(1+\nu)}{3E}\sigma^* \quad (21)$$

During the process of creep relaxation the total effective strain (sum of elastic and creep strains) at any point remains constant with time, that is

$$\varepsilon^* = \varepsilon_c^* + \varepsilon_e^* = \text{const} \quad (22)$$

Differentiating Eq. (22) with respect to time, one obtains

$$(d/dt)\varepsilon_e^* = -\dot{\varepsilon}_c^* \quad (23)$$

Substitution of Eqs. (18) and (21) into Eq. (23) results in

$$\frac{2}{3}\frac{1+\nu}{E}\frac{d}{dt}\sigma^* = -B\sigma^{*n}$$

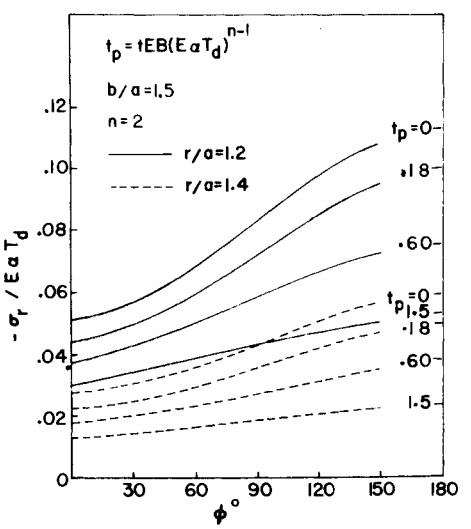

Fig. 2 Variation of radial stress with time for $n = 2$.

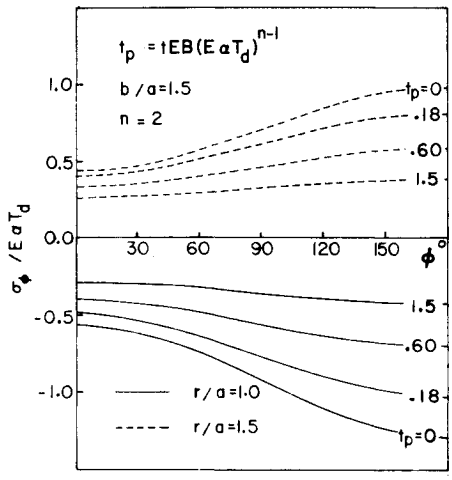

Fig. 3 Variation of tangential stress with time for $n = 2$.

or

$$\frac{d\sigma^*}{\sigma^{*n}} = -\frac{3}{2}\frac{BE}{1+\nu}dt \tag{24}$$

Now, integration of Eq. (24) in conjunction with the initial condition

$$\sigma^* = {\sigma_0}^* \quad \text{at} \quad t = 0 \tag{25}$$

yields

$$\sigma^* = \left[{\sigma_0}^{*(1-n)} - \frac{3}{2}\frac{1-n}{1+\nu}EBt\right]^{1/1-n} \tag{26}$$

Substituting the first of Eqs. (19) into (26), one obtains

$$(\sigma_\phi-\sigma_r)^2+(\sigma_r-\sigma_z)^2+(\sigma_z-\sigma_\phi)^2+6{\tau_{r\phi}}^2 = 2\left[{\sigma_0}^{*(1-n)} - \frac{3}{2}\frac{1-n}{1+\nu}EBt\right]^{2/1-n} \tag{27}$$

Simultaneous solution of Eqs. (20) and (27) and the equilibrium equations

$$\frac{\partial\sigma_r}{\partial r}+\frac{1}{r}\frac{\partial\tau_{r\phi}}{\partial\phi}+\frac{\sigma_r-\sigma_\phi}{r}=0$$
$$\frac{\partial\tau_{r\phi}}{\partial r}+\frac{1}{r}\frac{\partial\sigma_\phi}{\partial\phi}+\frac{2\tau_{r\phi}}{r}=0 \tag{28}$$

provides the time dependent stresses σ_r, σ_ϕ, σ_z, and $\tau_{r\phi}$.

The analytical solution of the preceding equations is not an easy task, particularly because n is a function of temperature. A numerical solution has, therefore, been attempted and the dimensionless results are plotted for the thermal boundary conditions shown in Fig. 1. The numerical procedure, however, is general and can be applied to any other creep relaxation problem. The following is an outline of the numerical technique.

1) Equation (26) is rearranged as

$$t = [{\sigma_0}^{*(1-n)} - \sigma^{*(1-n)}]\frac{2(1+\nu)}{3(1-n)EB} \tag{29}$$

and the solution region is divided into M and K sections in the radial and tangential directions, respectively.

2) The original stresses σ_{r_0}, σ_{ϕ_0}, σ_{z_0}, and $\tau_{r\phi_0}$ as well as the original effective stress ${\sigma_0}^*$ are calculated from Eqs. (15) and (16) and the first of Eqs. (19) for the nodal points $ij(i = 1, 2, 3, \ldots, M+1, j = 1, 2, 3, \ldots K+1)$.

3) A relaxation factor C_{ij} is assumed which at this stage is taken to be equal for all nodal points, that is

$$C_{11} = C_{12} = \cdots C_{1\,K+1} = \cdots C_{M+1\,K+1}$$

4) All original tangential stresses σ_{ϕ_0} calculated in step 2 are reduced by C_{ij} percent to obtain

$$\sigma_{\phi ij} = \sigma_{\phi_{0ij}}(1-C_{ij}) \tag{30}$$

Using the second equilibrium equation in Eq. (28) and the reduced tangential stresses $\sigma_{\phi ij}$, new values of shearing stresses for all nodal points are calculated by an iteration method. These new values of tangential and shearing stresses are then employed in conjunction with the first equilibrium equation in Eq. (28) and the boundary condition to obtain the radial stresses σ_{rij}.

Based on reduced σ_{rij} and $\sigma_{\phi ij}$ using Eq. (20), the reduced axial stresses σ_{zij} are calculated. The reduced stresses are then substituted into the first equation of Eqs. (19) to obtain the relaxed effective stress ${\sigma_{ij}}^*$ for each nodal point.

5) The time t_{ij} required for effective stress at each point to change from original, ${\sigma_{0ij}}^*$, to reduced value ${\sigma_{ij}}^*$ is calculated from Eq. (29).

6) The times, t_{ij}'s, are compared with t_{11} and if their differences are greater than some δ, a new value of C_{ij} is calculated for that point from

$$C_{ij_{\text{new}}} = C_{ij_{\text{old}}} \times (t_{11}/t_{ij}) \qquad i = 2, 3, \ldots M+1, \quad j = 2, 3, \ldots K+1 \tag{31}$$

Then Steps 4–6 are repeated.

7) After obtaining t_{ij}'s that all agree within the specified accuracy δ, the process is repeated for next increment of stress drop.

The results obtained for $b/a = 1.5$, $\beta = \pi/3$, $T_i > T_1 > T_2$ and various values of n are plotted in Figs. 2–10. In these figures, the actual time is replaced by a time parameter defined as

$$t_p = (E\alpha T_d)^{n-1}EBt_{\text{actual}} \tag{32}$$

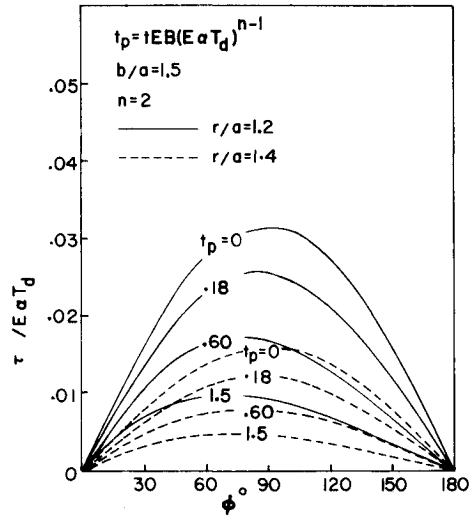

Fig. 4 Variation of shearing stress with time for $n = 2$.

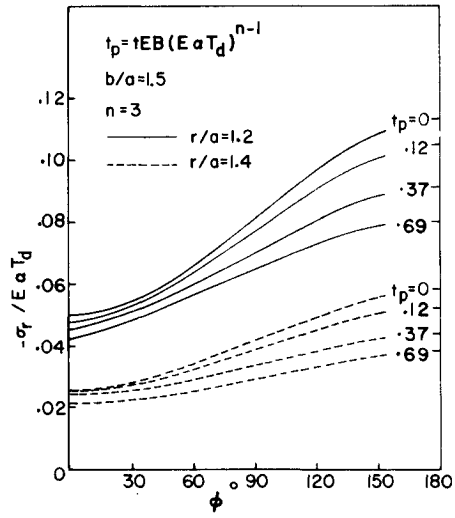

Fig. 5 Variation of radial stress with time for $n = 3$.

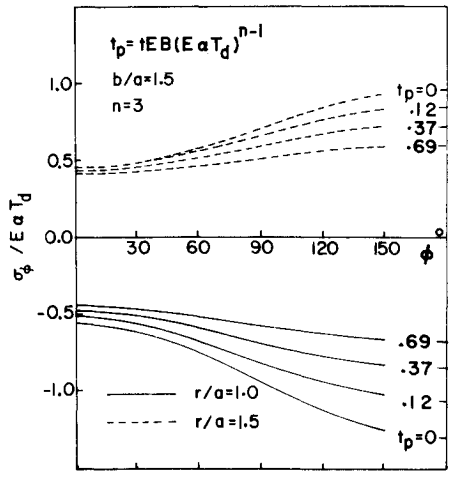

Fig. 6 Variation of tangential stress with time for $n = 3$.

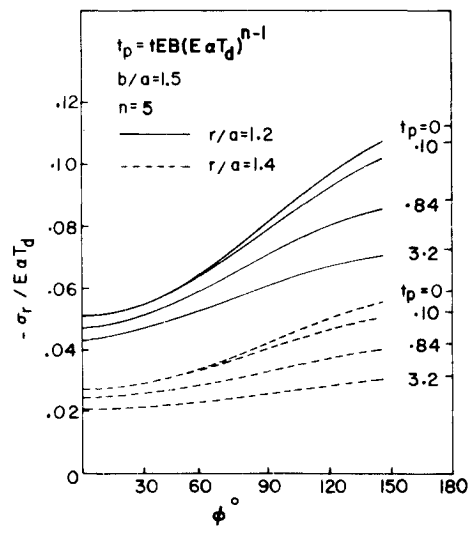

Fig. 8 Variation of radial stress with time for $n = 5$.

where

$$T_d = T_1 - T_2$$

In all of these figures, the curves $t_p = 0$ show the initial thermal stresses.

If the material's creep constant n is temperature dependent, n can be represented as follows

$$n_{ij} = n_1 + n_2(T_{ij} - T_2)/(T_1 - T_2) \tag{33}$$

where n_1 and n_2 are two positive constants. Using this temperature dependent n_{ij}, instead of a constant, the same procedure can be employed to calculate the relaxed thermal stresses. The only difference being that of calculating n_{ij}'s based on temperatures at the nodal points, T_{ij}, and using calculated n_{ij}'s in Eq. (29) at step 5.

Dimensionless results for temperature dependent n and, $b/a = 1.5$, $\beta = \pi/3$ are plotted in Figs. 11–16. In these figures, since n varies from one point to another, a different time parameter will have to be used. This time parameter is defined as

$$t_p = 10^{(4n_1 - 3)} EBt_{\text{actual}} \tag{34}$$

Discussion and Conclusion

The analytical solution of stress relaxation problems, involving combined state of stress, is usually associated with the solution of highly nonlinear and complicated partial differential equations. In the majority of cases, a closed form solution does not exist. The numerical method presented in this paper is a general approach that can be applied to other stress relaxation problems. The method converges relatively fast, although rate of

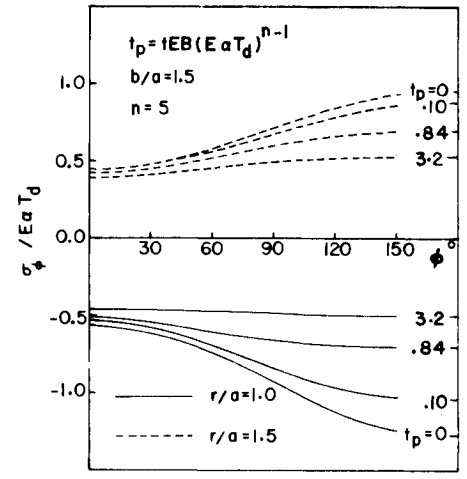

Fig. 9 Variation of tangential stress with time for $n = 5$.

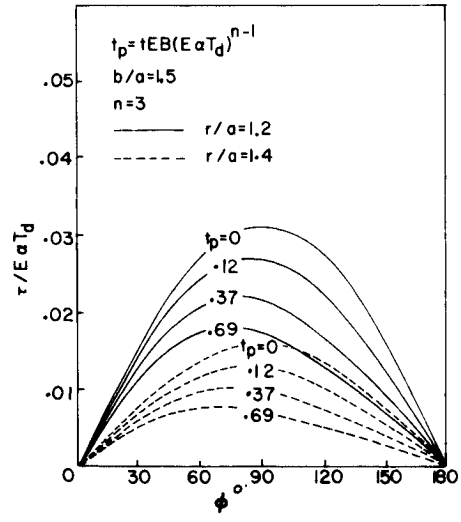

Fig. 7 Variation of shear stress with time for $n = 3$.

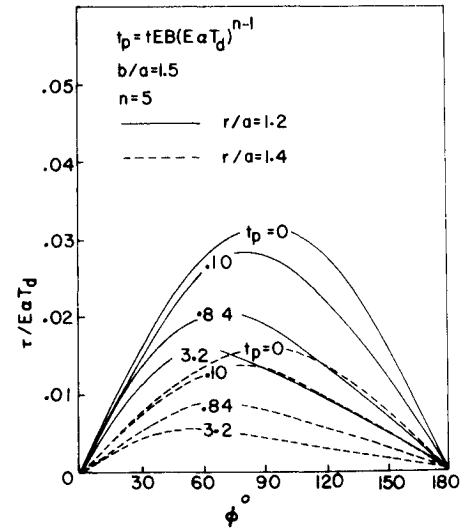

Fig. 10 Variation of shear stress with time for $n = 5$.

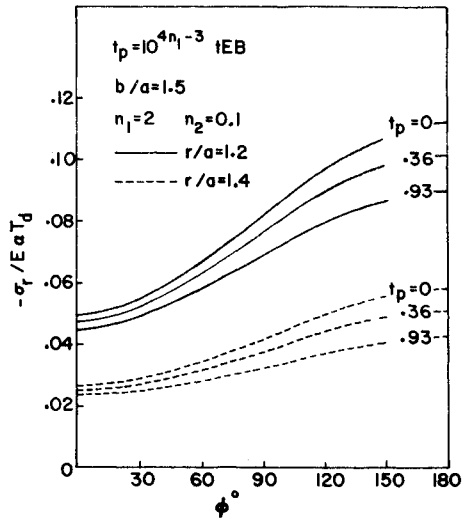

Fig. 11 Variation of radial stress with time for temperature dependent n ($n_1 = 2$, $n_2 = 0.1$).

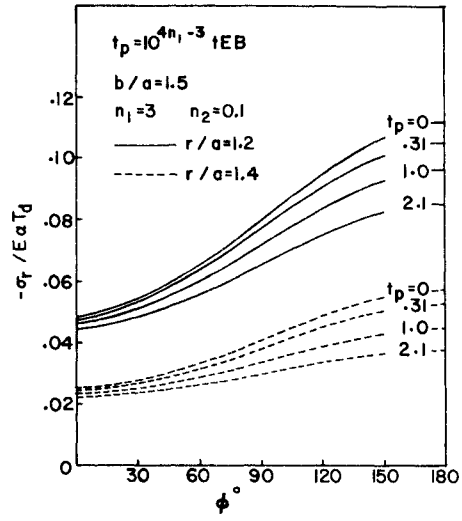

Fig. 14 Variation of radial stress with time for temperature dependent n ($n_1 = 3$, $n_2 = 0.1$).

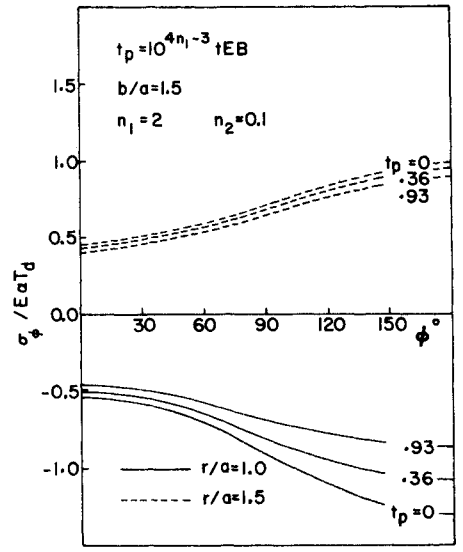

Fig. 12 Variation of tangential stress with time for temperature dependent n ($n_1 = 2$, $n = 0.1$).

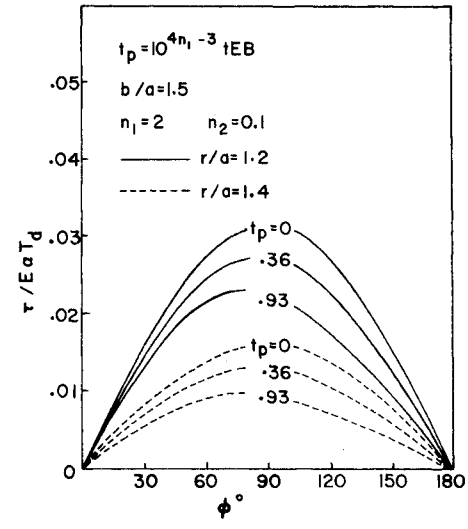

Fig. 13 Variation of shear stress with time for temperature dependent n ($n_1 = 2$, $n_2 = 0.1$).

convergence depends on the magnitude of relaxation factor C_{ij}, selected in step 2.

Figures 3, 6, and 9 show the tangential stresses at inner and outer boundaries for constant n's. In these figures, it can be seen that σ_ϕ increases at the outside and decreases at the inside of the cylinder as ϕ increases. This, of course, is expected considering that $T_i > T_1 > T_2$. The steepest change takes place at around $\phi = \beta$ where there is a discontinuity in temperature on the outside boundary. It can be noted on the same figures that the rate of relaxation is largest at $\phi = \pi$ simply because the magnitude of stresses at that point are largest. A similar conclusion can be drawn from Figs. 12 and 15 where they show the tangential stresses for the case of temperature dependent creep parameter n. A major difference that can be noticed between Figs. 3 and 12 as well as between Figs. 6 and 15 is that in Figs. 12 and 15 the rate of relaxation at the inner boundary ($r/a = 1$) is greater than that of outer boundary ($r/a = 1.5$). This is due to the fact that temperature at the inside is larger than the outside and since $n = n(T)$, it would have a larger value as r approaches a, therefore causing a greater rate of relaxation.

Figures 2, 5, and 8 show radial stresses for constant n and Figs. 11 and 14 show the same for temperature dependent n. These radial stresses are plotted for radii other than inside and outside, however, the same trends that were explained for tangential stresses can also be observed here.

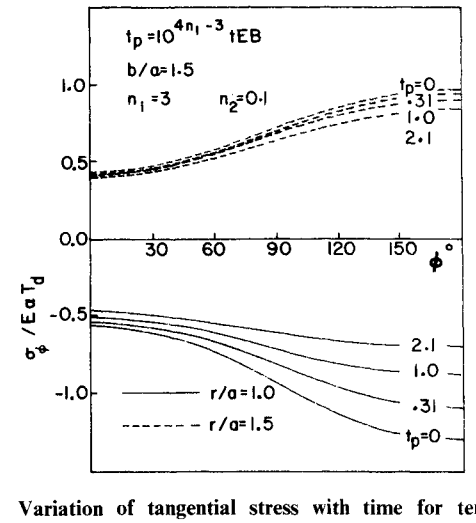

Fig. 15 Variation of tangential stress with time for temperature dependent n ($n_1 = 3$, $n = 0.1$).

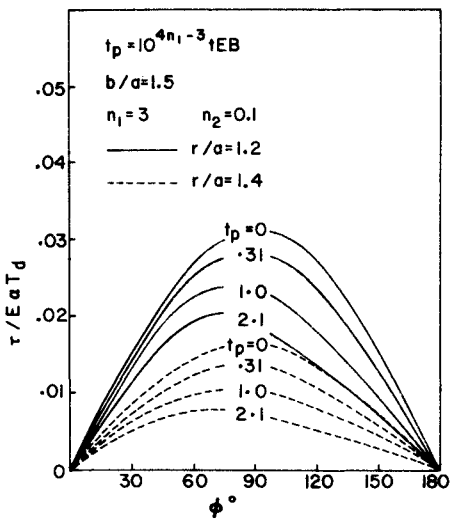

Fig. 16 Variation of shear stress with time for temperature dependent n ($n_1 = 3$, $n_2 = 0.1$).

The shearing stresses are plotted in Figs. 4, 7, 10, 13, and 16. In these figures it can be seen that the shearing stress which originally was symmetric about the axis $\phi = \pi/2$, becomes unsymmetric and its maximum tends to shift towards $\phi = \beta$. The original symmetry of shearing stress can probably be attributed to the domination of the effect $(T_i - T_2)$. But as stresses relax with time the shearing effect of $(T_1 - T_2)$ become dominant, thus causing the shift of shearing stress pick toward the point $\phi = \beta$.

The importance of inclusion of stress relaxation in design calculations becomes evident considering that when the cylinder is pressurized internally, tangential stress due to pressure would be tensile and maximum at the inside surface. Now if the inside temperature is greater than the outside temperature, the compressive tangential thermal stress will tend to reduce the intensity and effect of the former. While initially this favorable phenomenon exist, one should exercise care in taking advantage of this situation since thermal stresses relax with time but the stresses due to pressure basically remain the same. Thus, the stress at the inner surface of cylinder becomes more critical with time.

References

[1] Morozov, E. M. and Fridman, Y. B., "Strength and Deformation in Nonuniform Temperature Fields," *A Collection of Scientific Papers*, edited by Y. B. Fridman, Consultants Bureau, New York, 1964.

[2] Zudan, Z., Yen, T. C., and Steigelmann, W. H., *Thermal Stress Techniques in the Nuclear Industry*, Franklin Institute Research Laboratory, American Elsevier, New York, 1965.

[3] Boley, B. A. and Weiner, J. H., *Theory of Thermal Stresses*, Wiley, New York, 1960.

[4] Wahl, A. M., "Further Studies of Stress Distribution in Rotating Disks and Cylinders under Elevated Temperature Creep Conditions," *Journal of Applied Mechanics*, Vol. 25, No. 2, 1958.

[5] Baily, R. W., "Design Aspect of Creep," *ASME Transactions: Journal of Applied Mechanics*, Vol. 58, 1936, pp. A1–A6.

[6] Rabatnov, Yu. N., *Creep Problems in Structural Members*, Wiley, New York, 1969.

[7] McVetty, P. G., "Creep of Metals at Elevated Temperatures. The Hyperbolic Sine Relation between Stress and Creep Rate," *Transactions of the ASME*, Vol. 65, Oct. 1943, pp. 761–769.

[8] Nadai, A. and Davis, E. A., "The Creep of Metals II," *Journal of Applied Mechanics*, Sept. 1957.

[9] Grifith, I. E. and Marin, J., "Creep Relaxation for Combined Stress," *Journal of the Mechanics and Physics of Solids*, Vol. 4, No. 4, 1956.

[10] Sabbaghian, M., "Creep in Multilayered Shrink-Fitted Cylindrical Pressure Vessels," *Proceedings of the International Association for Shell Structures Symposium on Hydromechanically Loaded Shells*, 1971.

[11] Mendelson, A., *Plasticity: Theory and Application*, Macmillan, New York, 1968.

[12] Sabbaghian, M. and Eslami, M. R., "Creep Relaxation of Axisymmetric Thermal Stresses in Thick Walled Cylindrical Vessels," ASME Paper 74-PVP-9, presented at the ASME Pressure Vessel and Piping Conference, Miami Beach, Fla., 1974.